

Electrochemical Behaviors of Myoglobin on Ionic Liquid-Graphene-Cobalt Oxide Nanoflower Composite Modified Electrode and Its Electrocatalytic Activity

Sheng Kang, Wenshu Zhao, Xiaoyan Li, Zuorui Wen, Xueliang Niu, Bolin He, Linfang Li, Wei Sun*

Key Laboratory of Tropical Medicinal Plant Chemistry of Ministry of Education, College of Chemistry and Chemical Engineering, Hainan Normal University, Haikou 571158, P R China,

*E-mail: swyy26@hotmail.com

Received: 18 December 2016 / Accepted: 29 January 2017 / Published: 12 February 2017

A biocomposite was prepared by mixing myoglobin (Mb), ionic liquid (IL) 1-butyl-3-methylimidazolium tetrafluoroborate, graphene (GR) and cobalt oxide (Co₃O₄) nanoflower together. Then the mixture was applied on carbon ionic liquid electrode (CILE) to get a modified electrode with chitosan film. Ultraviolet-visible and FT-IR spectroscopic experiments showed that Mb in the composite remained its native structure. On cyclic voltammogram a pair of well-defined redox peaks was got in 0.1 mol L⁻¹ pH 5.0 phosphate buffer solution, which was ascribed to the realization of direct electrochemistry of Mb with the underlying electrode. The synergistic effects of IL, GR and Co₃O₄ nanoflower provided a fast electron transfer path for the movement of electron from Mb active centers to the electrode. Electrochemical parameters of electrode reaction of Mb were calculated. The Mb modified electrode showed excellent electrocatalytic ability towards the reduction of trichloroacetic acid, which indicated that a new third-generation electrochemical biosensor was constructed successfully.

Keywords: Myoglobin; Ionic liquid; Graphene; Cobalt oxide nanoflower; Electrochemical biosensor

1. INTRODUCTION

Direct electrochemical investigations of redox proteins/enzymes can be used to construct a model for mechanism research on enzymes in biological systems [1], and the result can explain the relationship of the structure and function. Also the investigation on direct electron exchange from proteins to electrodes can be used as platform to prepare biosensors or enzymatic bioreactors [2]. Various protein modified electrodes have been fabricated to fasten electron transfer rate of redox proteins to the basic electrodes. The presence of modifiers forms a biocompatible interface to remain the molecular structure and biocatalytic activity [3]. The immobilized redox enzymes on electrodes

often have an enhanced electron transfer rate with excellent electrochemical responses appeared due to the effects of the modifiers used. Zheng et al. investigated direct electrochemistry of horseradish peroxidase on MoS₂ nanosheet modified electrode [4]. Liu et al. realized direct electron transfer of hemoglobin immobilized on two-dimensional layered Ti₃C₂-based material [5]. Yan et al. studied direct electrochemistry of myoglobin (Mb) with electrodeposited TiO₂ and alginate composite modified electrode [6].

Ionic liquids (ILs) are organic salts that consisted of ions, which exhibit the physicochemical characteristics such as fast ionic conductivity, wide electrochemical windows and good solubility [7]. Therefore various ILs have been used in electrochemistry and electroanalysis [8]. Wei et al. summarized the usage of ILs in electrochemical sensors [9]. Due to the excellent solubility ILs are acted as the supporting electrolyte and the binder/modifier in electrochemical investigation. IL based carbon paste electrode, which is called as carbon ionic liquid electrode (CILE), is widely used as the basic working electrode for electroanalytical detections [10, 11]. CILE has showed excellent electrochemical performances including electrocatalytic activity, good anti-fouling ability and stable electrochemical responses [12-14].

As a monolayer of sp² hybridized carbon atoms, graphene (GR) has attracted enormous attentions due to the properties of fast conductivity, excellent mechanical and electronic properties, which has wide applications in electrochemical sensors and catalysis [15]. Recently GR-based composites have been developed for constructing electrochemical sensors, which exhibit advanced performance due to the synergistic effects [16]. Nanosized metal oxides own the characteristics including less-toxicity, good biocompatibility, easy synthesis procedure, chemical stability, excellent electrocatalytic activity, which have been used in the protein electrochemistry. Various metal oxides including zirconium oxide [17], titanium oxide [18] and zinc oxide [19] etc. had been successfully applied to enzymes immobilization for the fabrication of biosensor. Recently GR and Co₃O₄ nanocomposite had been synthesized and used for the electrochemical applications [20, 21]. However, no references have been published with IL, GR and Co₃O₄ nanoflower for the protein electrochemistry.

In the present report a new bionanocomposite was got by simply mixing Mb, 1-butyl-3-methylimidazolium tetrafluoroborate (BMIMBF₄), GR and Co₃O₄ nanoflower together. Then it was casted on CILE surface with a chitosan (CTS) film for fixation. Direct electrochemistry of Mb within nanocomposite was investigated, which gave a pair of well-defined quasi-reversible redox peaks. This Mb based sensor exhibited excellent electrocatalytic ability to trichloroacetic acid (TCA) reduction with better sensitivity, which proved the successful fabrication of a new electrochemical sensing platform.

2. EXPERIMENTAL

2.1 Apparatus and reagents

BMIMBF₄ (Lanzhou Yulu Fine Chemical Co. Ltd., China), bovine Mb (MW. 16800, Sigma-Aldrich Co., USA), graphene (GR, Nanjing XFNano Materials Tech. Ltd. Co., China), graphite

powder (average particle size 30 μm , Shanghai Colloid Chem. Co., China), $\text{Co}(\text{NO}_3)_2 \cdot 6\text{H}_2\text{O}$ (National Pharmaceutical Group Chem. Reagent Ltd. Co., China), CTS (Dalian Xindie Chem. Ltd. Co., China) and TCA (Tianjin Kemiou Chem. Ltd. Co., China) were used as received. 0.1 mol L^{-1} phosphate buffer solutions (PBS) was selected as the supporting electrolyte. Co_3O_4 nanoflowers were synthesized according to the reference [22]. All the chemicals were of analytical reagent grade and doubly distilled water was used in the experiments.

A CHI 440A electrochemical workstation (Shanghai CH Instrument, China) was employed for the electrochemical measurements with a three-electrode model. Mb modified electrode was acted as working electrode. A platinum wire electrode was auxiliary electrode and a saturated calomel electrode (SCE) was reference electrode. Ultraviolet-visible (UV-Vis) absorption spectrum was performed on Cary 50 probe spectrophotometer (Varian, Australia) with FT-IR spectrum on Tensor 27 FT-IR spectrophotometer (Bruker, Germany). Scanning electron microscopy (SEM) was carried out on a JSM-6700F scanning electron microscope (Japan Electron Company, Japan). X-ray powder diffraction (XRD) pattern was operated on a Japan RigakuD/Maxr-A X-ray diffractometer with graphite monochromatized high-intensity $\text{Cu K}\alpha$ radiation ($\lambda=1.54178\text{\AA}$).

2.2 Preparation of modified electrode

IL modified carbon paste was hand-mixed with 0.10 mL $[\text{BMIM}]\text{BF}_4$, 0.90 mL liquid paraffin and 3.2 g graphite powder in a mortar. Then the paste was inserted in a glass electrode tube ($\Phi = 4 \text{ mm}$) with copper wire as electrical contact. The CILE surface was smoothed on a weighing paper just before use.

The modifier was got by mixing 12.0 mg Mb, 60 μL BMIMBF_4 , 75 μL 2.0 L^{-1} GR and 100 μL 1.0 mg L^{-1} Co_3O_4 nanoflower together, which was diluted to 1.0 mL by PBS (pH 7.0). After sonicated homogeneously, 8.0 μL Mb-IL-GR- Co_3O_4 mixture was dropped on CILE and dried at room temperature. Finally 8.0 μL CTS (1.0 mg mL^{-1} in 1% HAc solution) was casted on the electrode surface and dried to get a stable membrane. The resulted electrode was named as CTS/Mb-IL-GR- Co_3O_4 /CILE and put in $4 \text{ }^\circ\text{C}$ refrigerator when not in use. Other electrodes were fabricated by the similar procedure for comparison.

2.3 Procedure

Electrochemical experiments were performed in a 10 mL electrochemical cell with 0.1 mol L^{-1} PBS as the supporting electrolyte, which was deoxygenated by N_2 for 30 min before experiments with N_2 environment kept in the experiments. UV-Vis spectroscopy was done with a CTS, Mb, BMIMBF_4 , GR and Co_3O_4 nanoflower mixture solution. The Mb-IL-GR- Co_3O_4 mixture was dropped on a glass slide and dried for FT-IR.

3. RESULTS AND DISCUSSION

3.1 SEM and XRD of composite materials

Fig. 1a showed the morphology of the prepared Co_3O_4 nanoflower, which was composed of nanosheets with many holes (inset of Fig. 1a). The Co_3O_4 nanoflower had large surface area with porous structure, which provided valid space for the enzyme immobilization. Fig. 1b was the XRD result of Co_3O_4 nanoflower. All the diffraction peaks could be indexed to the standard raw salt cubic Co_3O_4 with the lattice constant (a) as 8.0650 Å, which was consistent with the value in the standard card (JCPDS card no. 74-1656) without other peaks of impurities. As for Mb-IL-GR- Co_3O_4 composite (Fig. 1c and d), the thickness of layer structure increased apparently with the flower structure still remained, which proved the successful preparation of the nanocomposite with good homogeneity.

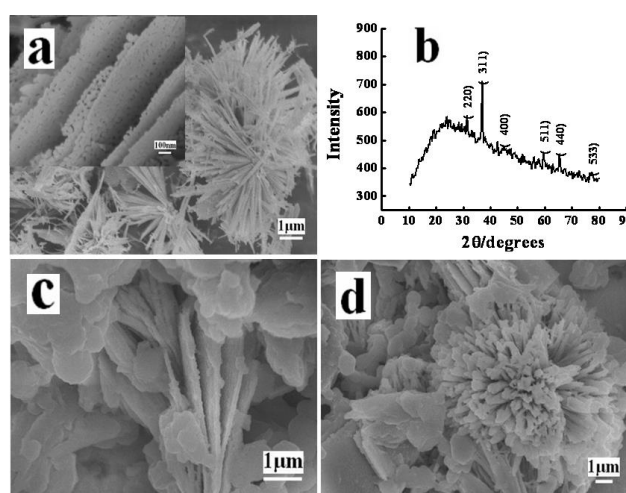


Figure 1. SEM images of (a) Co_3O_4 nanoflower (inset was the enlarged image), (b) XRD of Co_3O_4 nanoflower, (c, d) SEM images of Mb-IL-GR- Co_3O_4 composite with different magnitude.

3.2 Spectroscopic results

The Soret absorption of redox enzymes in UV-Vis absorption spectrum can be used to prove the conformational integrity. If heme region is denaturation with conformational change, the Soret band will move [23]. As shown in Fig. 2A, the Soret band of Mb (409.0 nm, curve a) was the same as that of Mb mixed with the materials single or totally (curves b to e), indicating that Mb in the composite kept the native structure due to the biocompatibility of CTS, IL, GR and Co_3O_4 nanoflower that used.

FT-IR spectroscopy is another tool to check the secondary conformation of protein. The shape and position of amide I and II infrared absorbance bands can reflect the structure information of the polypeptide chain. The denatured protein will result in the diminishment even disappearance of the related bands [24]. In Fig. 2Ba the amide I and amide II of Mb appeared at 1647 cm^{-1} and 1568 cm^{-1} ,

which was the same as that mixed with IL-GR- Co_3O_4 (1646 cm^{-1} and 1568 cm^{-1} , Fig. 2Bb). Therefore the native structure of Mb in the mixture remained unchanged.

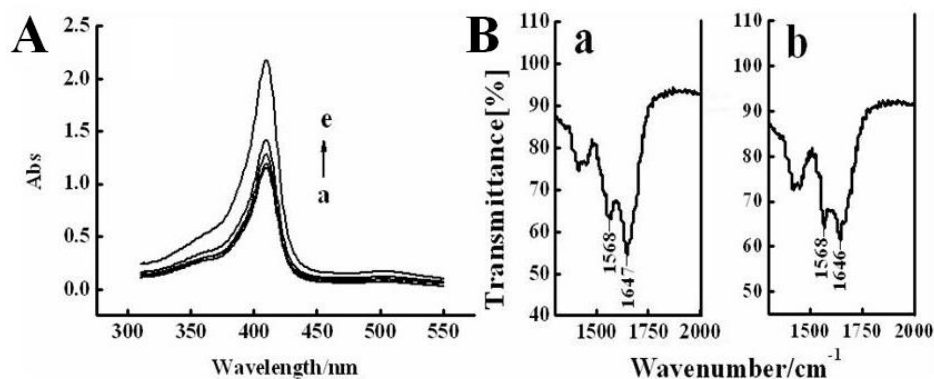


Figure 2. (A) UV-Vis absorption spectra of Mb in (a) CTS, (b) CTS-IL-GR, (c) CTS-IL- Co_3O_4 , (d) CTS-GR- Co_3O_4 and (e) CTS-IL-GR- Co_3O_4 mixture; (B) FT-IR spectra of (a) Mb and (b) Mb-IL-GR- Co_3O_4 mixture.

3.3 Electrochemical characteristics of the modified electrode

Electrochemical characteristics of different modified electrodes were checked by cyclic voltammetry with potassium ferricyanide as probe and the data was shown in Fig. 3. The redox peak of ferricyanide changed greatly on different electrodes with the current sequence from low to high as CTS/Mb/CILE (curve a), CTS/Mb-GR/CILE (curve b), CTS/Mb-GR- Co_3O_4 /CILE (curve c), CTS/Mb-IL- Co_3O_4 /CILE (curve d) and CTS/Mb-IL-GR- Co_3O_4 /CILE (curve e). The gradually increment of the redox peak current was ascribed to the increase of the interfacial conductivity, which was benefit for the electron transfer of ferricyanide. The incorporation of high conductive IL, GR and semi-conductive Co_3O_4 nanoflower step-by-step can change the whole interfacial conductivity with the electron transfer rate enhanced.

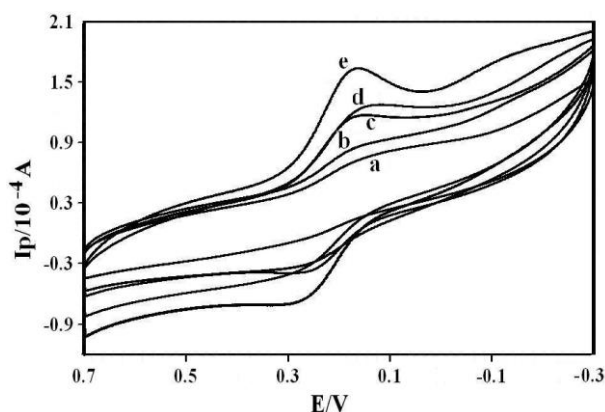


Figure 3. Cyclic voltammograms of (a) CTS/Mb/CILE, (b) CTS/Mb-GR/CILE, (c) CTS/Mb-GR- Co_3O_4 /CILE, (d) CTS/Mb-IL- Co_3O_4 /CILE, (e) CTS/Mb-IL-GR- Co_3O_4 /CILE in a mixture solution of 10.0 mmol L^{-1} $[\text{Fe}(\text{CN})_6]^{3-/4-}$ and 0.1 mol L^{-1} KCl with scan rate as 100 mV s^{-1} .

3.4 Direct electrochemistry of the Mb modified electrode

Cyclic voltammetric results of different electrodes in deoxygenated PBS were listed in Fig. 4. On CILE (curve a) no responses appeared with stable background current. On CTS/Mb/CILE (curve b) a pair of small and unsymmetrical redox peaks was observed, proving a quasi-reversible electrochemical reaction with slow electron transfer rate. On CTS/Mb-IL-GR- Co_3O_4 /CILE (curve c) the redox peak currents increased obviously, which could be ascribed to the synergistic effects of the substances, including large porous structure of Co_3O_4 nanoflower, fast conductivity of GR and IL, and the advantages of CILE. Therefore a favorable three-dimensional nanostructure was formed for the Mb immobilization, which was benefit for the electron transfer of Mb. From curve c the potential values were got as -0.289 V (E_{pc}) and -0.203 V (E_{pa}). The apparent formal potential ($E^{0'}$) from the average of the redox peak potentials, was -0.246 V, which was the characteristic of the Mb heme Fe(III)/Fe(II) redox couples. The peak-to-peak separation (ΔE_p) was got as 0.086 V and the ratio of I_{pc}/I_{pa} was nearly to 1, indicating a quasi-reversible electrochemical process from Mb reaction.

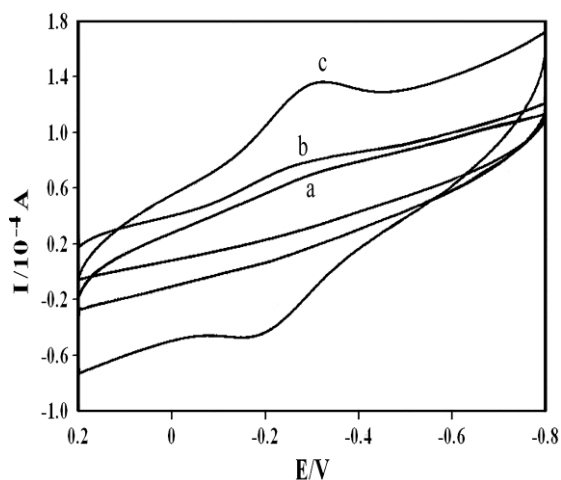


Figure 4. Cyclic voltammograms of (a) CILE, (b) CTS/Mb/CILE and (c) CTS/Mb-IL-GR- Co_3O_4 /CILE in pH 5.0 PBS at the scan rate of 100 mV s^{-1} .

3.5 Electrochemical investigation

The influence of scan rate on the electrochemistry of CTS/Mb-IL-GR- Co_3O_4 /CILE was recorded and shown in Fig. 5. The increase of scan rate resulted in the appearance of symmetric redox peaks with almost same peak currents and the increase of ΔE_p value, proving a quasi-reversible process. Therefore the electroactive Mb Fe(III) was reduced to Mb Fe(II) on the forward scan, which was reoxidized to Mb Fe(III) on the reverse scan. The peak currents increased linearly with scan rate from 100 to 700 mV s^{-1} (inset A of Fig. 5), indicating a surface-controlled thin-layer process. As shown in inset B of Fig. 5, two straight lines were got with the equations as $E_{pc}(\text{V}) = -0.048 \ln v - 0.39$ ($\gamma = 0.996$) and $E_{pa}(\text{V}) = 0.020 \ln v - 0.17$ ($\gamma = 0.997$). Then electrochemical parameters were got with the Laviron's equation [25]. The electron transfer coefficient (α) and the apparent heterogeneous electron

transfer rate constant (k_s) were got as 0.437 and 0.675 s^{-1} . This k_s value was higher than some reported values such as Nafion-Mb-BMIMPF₆/CPE (0.36 s^{-1}) [26], Nafion/Mb/Co/CILE (0.588 s^{-1}) [27], Mb-HSG-SN-CNTs/GCE (0.41 s^{-1}) [28], CTS-Mb-GR-IL/CILE (0.652 s^{-1}) [29], Nafion/Mb-GR-Pt/CILE (0.584 s^{-1}) [30]. Therefore electron transfer of Mb was fast within three-dimensional structure of CTS/IL-GR-Co₃O₄ composite. The surface concentration (Γ^*) of Mb involved in the reaction was got by the integration of reduction peaks with the equation $Q=nFA\Gamma^*$ [31] and the value (6.81×10^{-8} mol cm^{-2}) was bigger than the theoretical monolayer value (1.89×10^{-11} mol cm^{-2}) [32]. Therefore multilayer of Mb took part in the electron transfer because of the specific flowerlike three-dimensional structure formed on the electrode surface.

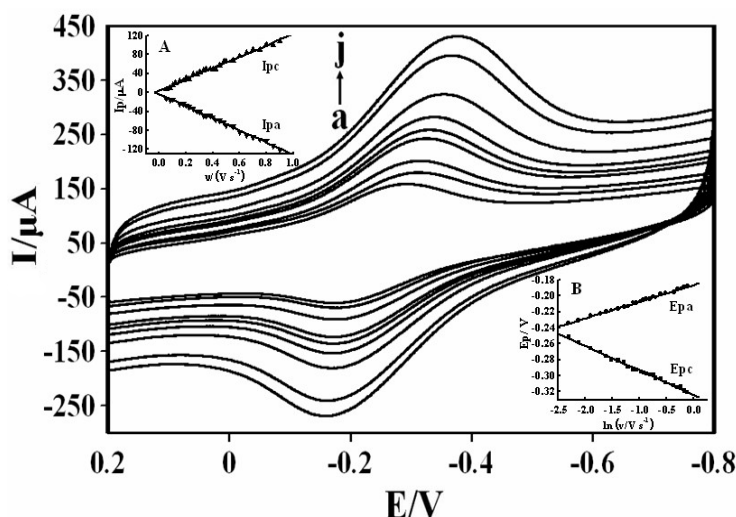


Figure 5. Cyclic voltammograms of CTS/Mb-IL-GR-Co₃O₄/CILE in pH 5.0 PBS at different scan rates (from a to j: 100,120, 150, 200, 250, 300, 400, 500, 600,700 $mV s^{-1}$). Inset A: Linear relationship of I_{pc} and I_{pa} versus scan rate; inset B: Linear relationship of E_{pa} and E_{pc} versus $\ln v$.

3.6 Electrocatalytic activity

This Mb based sensor had good electrocatalytic ability to the TCA reduction with cyclic voltammograms for different amounts of TCA shown in Fig. 6. The increase of TCA concentrations led to a significant enhancement of the reduction peak current along with the decrease of the oxidation peak, showing a typical electrocatalytic reaction. The reduction currents increased with TCA concentration from 1.0 to 20.0 $mmol L^{-1}$ with the linear regression equation as $I_{ss} (\mu A) = 46.75 C (mmol L^{-1}) + 379.91$ ($\gamma = 0.997$) and the detection limit as 0.18 $mmol L^{-1}$ (3σ). When the amount of TCA was larger than 20.0 $mmol L^{-1}$, the current reached a stable value, which obeyed a Michaelis-Menten kinetic process. Then the apparent Michaelis-Menten constant (K_M^{app}) was got as 0.98 $mmol L^{-1}$ by the electrochemical expression of Lineweaver-Burk equation [33]. A systematic comparison of this Mb based electrochemical biosensor for TCA detection with other previous works was summarized in Table 1. A relatively wider dynamic range and smaller detection limit were achieved, demonstrating that IL-GR-Co₃O₄ composite was beneficial for the preparation of Mb sensor.

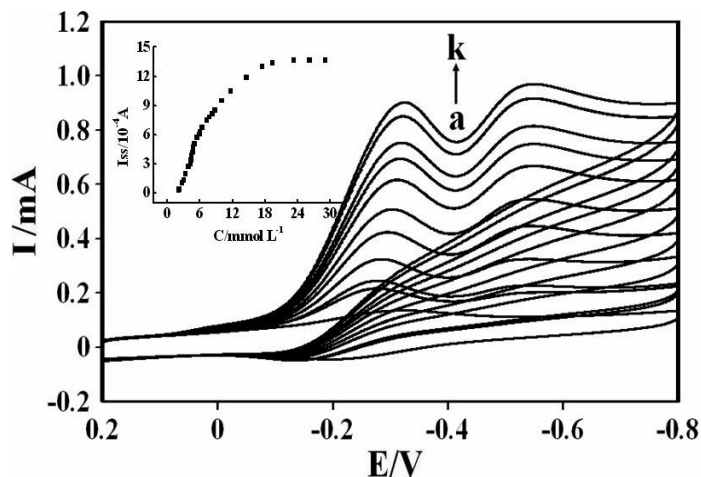


Figure 6. Cyclic voltammograms of CTS/Mb-IL-GR-Co₃O₄/CILE in 0.1 mol L⁻¹ pH 5.0 PBS with 0, 2.5, 3.3, 3.5, 4.0, 4.2, 4.5, 5.0, 5.3, 6.0, 7.0 mmol L⁻¹ TCA (curve a-k) at the scan rate of 100 mV s⁻¹. Inset: relationship of catalytic reduction peak currents and the TCA concentration.

Table 1. Comparisons of the analytical parameters for TCA detection by Mb based biosensors.

Modified electrodes	Linear range (mmol L ⁻¹)	Detection limit (mmol L ⁻¹)	K_M^{app} (mmol L ⁻¹)	Refs.
Nafion/Mb-SA-TiO ₂ /CILE	5.3-114.2	0.152	32.3	[6]
Nafion-BMIMPF ₆ /Mb/CPE	0.2-11.0	0.016	-	[26]
Nafion/Mb/Co/CILE	0.4-12.0	0.2	4.11	[27]
CTS-Mb-GR-IL/CILE	2.0-16.0	0.583	8.99	[29]
Nafion/Mb-GR-Pt/CILE	0.9-9.0	0.32	0.126	[30]
CTS/Mb/GR-ZnO/CILE	0.4-53.0	0.10	1.64	[34]
Nafion/Mb-Co ₃ O ₄ -Au/IL-CPE	2.0-20.0	0.5	4.70	[35]
Nafion-BMIMPF ₆ /Mb/CILE	1.6-19.6	0.2	90.8	[36]
Nafion/Mb/NiO/GR/CILE	0.69-30.0	0.23	10.67	[37]
CTS/Mb-IL-GR-Co ₃ O ₄ /CILE	1.0-20.0	0.18	0.98	This Work

SA: sodium alginate, BMIMPF₆: 1-butyl-3-methylimidazolium hexafluorophosphate, CPE: carbon paste electrode.

3.7 Stability and repeatability

The stability of CTS/Mb-IL-GR-Co₃O₄/CILE was investigated by recording the multi-cyclic voltammetric scanning for 60 cycles, which resulted in no decrease of the response. The storage stability was checked by putting the electrode in 4 °C refrigerator. 98.6 % of the initial response was remained after 14 days storage and the current decreased for 8.3 % after 30 days. The excellent stability was attributed to the biocompatibility of the composite that retained the structure and

electrochemical activity of Mb. Nine Mb modified electrodes were fabricated by the same method independently and use for the determination of 5.0 mmol L⁻¹ TCA. The relative standard deviation (RSD) was got as 2.4 %, indicating the good repeatability.

3.8 Analytical application

With the purpose of evaluating the real applications of CTS/Mb-IL-GR-Co₃O₄/CILE, the analysis of TCA content in lab water samples were done with the results listed in Table 2. No TCA residues could be found in the lab water and the recovery was obtained within the range of 97.0 %-103.7 % by the standard addition method with the RSD less than 5%. Therefore the Mb modified electrode was able to determinate TCA content with satisfactory results.

Table 2. Determination of TCA in the water samples (n=3)

Water Sample	Found (mmol L ⁻¹)	Added (mmol L ⁻¹)	Found (mmol L ⁻¹)	Recovery (%)	RSD (%)
1	0	5.0	4.85	97.0	2.92
2	0	10.0	10.20	102.0	3.26
3	0	15.0	15.56	103.7	4.53

4. CONCLUSIONS

In the paper a composite of Mb, IL, GR and Co₃O₄ nanoflower was prepared for the modification of CILE to obtain an electrochemical Mb sensor. Spectroscopic data showed that Mb in the composite retained its structure. Electrochemical data proved that direct electron transfer of Mb in the composite was accelerated due to the synergistic effects of the materials, including the porous and three-dimensional structure of Co₃O₄ nanoflower, the high conductivity of ILs and GR, the biocompatibility and film forming ability of CTS, and the excellent characteristics of CILE. The Mb modified electrode can be used for electrocatalysis to the reduction of TCA, which had the potential applications in biosensor and biocatalysis.

ACKNOWLEDGEMENTS

We acknowledge the financial support of the National Natural Science Foundation of China (21365010), the International Science and Technology Cooperation Project of Hainan Province (KJHZ2015-13), the Program for Innovative Research Team in University (IRT-16R19) and the Science and Research Key Project of Universities of Hainan Province (Hnky2016ZD-10).

References

1. F.W. Scheller, N. Bistolas, S.Q. Liu, M. Jänchen, M. Katterle and U. Wollenberger, *Adv. Colloid Interface*, 116 (2005) 111.
2. P. Bianco, *J. Biotechnol.*, 82 (2002) 393.
3. S.A. Bhakta, E. Evans, T.E. Benavidez and C.D. Garcia, *Anal. Chim. Acta*, 872 (2015) 7.
4. W. Zheng, G.J. Li, L.H. Liu, W. Chen, W.J. Weng and W. Sun, *Int. J. Electrochem. Sci.*, 11 (2016) 7584.
5. H. Liu, C.Y. Duan, C.H. Yang, W.Q. Shen, F. Wang and Z.F. Zhu. *Sensor. Actuat. B-Chem.*, 218 (2015) 60.

6. H.Q. Yan, X.Q. Chen, Z.F. Shi, Y.H. Feng, J.C. Li, X.H. Wang and W. Sun. *J. Solid State Electr.*, 20 (2016) 1783.
7. M. Galiński, A. Lewandowski and I. Stepniak, *Electrochim. Acta*, 51 (2006) 5567.
8. W. Sun, R.F. Gao and K. Jiao, *Chinese J. Anal. Chem.*, 35 (2007) 1813.
9. D. Wei and A. Ivaska, *Anal. Chim. Acta*, 607 (2008) 126.
10. N. Maleki, A. Safavi, F. Sedaghati and F. Tajabadi, *Anal. Biochem.*, 369 (2007) 149.
11. J.B. Zheng, Y. Zhang and P.P. Yang, *Talanta*, 73 (2007) 920.
12. X.L. Niu, L.J. Yan, X.B. Li, A.H. Hu, C.J. Zheng, Y.L. Zhang and W. Sun, *Int. J. Electrochem. Sci.*, 11 (2016) 1720.
13. X.L. Niu, L.J. Yan, X.B. Li, Z.R. Wen, J.H. Yu, A.H. Hu, L.F. Dong, Z.F. Shi and W. Sun, *Int. J. Electrochem. Sci.*, 11 (2016) 7139.
14. S. Momeni, M. Farrokhnia, S. Karimi and I. Nabipour, *J. Iran. Chem. Soc.*, 13 (2016) 1027.
15. J.Q. Liu, Z. Liu, C.J. Barrow and W.R. Yang, *Anal. Chim. Acta*, 859 (2015) 1.
16. X.Q. Yu, W.S. Zhang, P.P. Zhang and Z.Q. Su, *Biosens. Bioelectron.*, 89 (2016) 72
17. W.C. Wang, X.Q. Li, X.H. Yu, L.J. Yan, B.X. Lei, P. Li, C.X. Chen and W. Sun, *J. Iran. Chem. Soc.*, 13 (2016) 323.
18. W. Sun, X.Q. Li and K. Jiao, *J. Chin. Chem. Soc.*, 55 (2008) 1074.
19. W. Sun, Z.Q. Zhai, D.D. Wang, S.F. Liu and K. Jiao, *Bioelectrochemistry*, 74 (2009) 295.
20. X.L. Sun, Z.Q. Jiang, C.X. Li, Y.Y. Jiang, X.Y. Sun, X.N. Tian, L.J. Luo, X.G. Hao and Z.J. Jiang. *J. Alloy. Compd.*, 685 (2016) 507.
21. G.P. Dai, P. Lu, Y. Liang and Y.T. Lei. *J. Chin. Chem. Soc.*, 60 (2013) 366.
22. J. Jiang, J.P. Liu, R.M. Ding, X.X. Ji, Y.Y. Hu, X. Li, A.Z. Hu, F. Wu, Z.H. Zhu and X.T. Huang, *J. Phys. Chem. C*, 114 (2010) 929.
23. J.F. Rusling and A.E.F. Nassar, *J. Am. Chem. Soc.*, 115 (1993) 11891.
24. J.K. Kauppinen, D.J. Moffatt, H.H. Mantsch and D.G. Cameron, *Appl. Spectrosc.*, 35 (1981) 271.
25. E. Laviron, *J. Electroanal. Chem.*, 52 (1974) 355.
26. X.Q. Li, R.J. Zhao, Y. Wang, X.Y. Sun, W. Sun, C.Z. Zhao and K. Jiao, *Electrochim. Acta*, 55 (2010) 2173.
27. W. Sun, X.Q. Li, P. Qin and K. Jiao, *J. Phys Chem. C.*, 113 (2009) 11294.
28. C.Y. Liu and J.M. Hu, *Biosens. Bioelectron.*, 24 (2009) 2149.
29. C.X. Ruan, T.T. Li, Q.J. Niu, M. Lu, J. Lou, W.M. Gao and W. Sun, *Electrochim. Acta*, 64 (2012) 183.
30. W. Sun, L.F. Li, B.X. Lei, T.T. Li, X.M. Ju, X.Z. Wang, G.J. Li and Z.F. Sun, *Mat. Sci. Eng. C-Mater.*, 33 (2013) 1907.
31. A.J. Bard and L.R. Faulkner, *Electrochemical methods: fundamentals and applications*. Wiley: New York, 1980.
32. S.F. Wang, T. Chen, Z.L. Zhang, D.W. Pang and K.Y. Wong, *Electrochem. Commun.*, 9 (2007) 1709.
33. R.A. Kamin and G.S. Wilson, *Anal. Chem.*, 52 (1980) 1198.
34. L.J. Yan, W.C. Wang, B.X. Lei, J.W. Xi, P. Li, L. Liu, X. Zhang and W. Sun, *Sensor Lett.*, 14 (2016) 39.
35. X. F. Wang, Z. You, H. L. Sha, S. X. Gong, Q. J. Niu and W. Sun, *Microchim. Acta*, 181 (2014) 767.
36. W. Sun, X. Q. Li and K. Jiao, *Electroanal.*, 21 (2009) 959.
37. W. Sun, S. X. Gong, Y. Deng, T. T. Li, Y. Cheng, W. C. Wang and L. Wang, *Thin Solid Films*, 562 (2014) 653.